International Immunopharmacology 66 (2019) 127–138

Contents lists available at ScienceDirect

International Immunopharmacology

journal homepage: www.elsevier.com/locate/intimp

PD-1 blockade augments humoral immunity through ICOS-mediated CD4$^+$ T cell instruction

Meiyu Zhang[a], Liliang Xia[a], Yi Yang[b], Shuai Liu[a], Ping Ji[a], Shujun Wang[a], Yingying Chen[a], Zhiduo Liu[a], Yanyun Zhang[a], Shun Lu[b], Ying Wang[a,*]

[a] Shanghai Institute of Immunology, Department of Immunology and Microbiology, Shanghai Jiao Tong University School of Medicine, Shanghai, China
[b] Shanghai Chest Hospital, Shanghai Jiao Tong University, Shanghai, China

ARTICLE INFO

Keywords:
PD-1 blockade
Humoral immunity
Germinal center
CD4$^+$ T cells
ICOS
ERK activation

ABSTRACT

Successful applications of PD-1/PD-L1 blockade in multiple cancers highlight the efficacy of immunotherapy mediated by enhancing CD8$^+$ T cell immunity both in mouse and human. How PD-1 blockade affects humoral immunity remains unclear. Herein we demonstrated that treatment of anti-PD-1 antibody led to the increase in both total IgG and OVA-specific IgG in OVA-immunized mice. However, no effect was observed on Ab affinity maturation. Accumulation of germinal center (GC) and memory B cells was observed in the spleens together with elevated percentages of plasma cells in the spleens and bone marrow. More interestingly, dramatic infiltration of CD4$^+$ T cells was apparent in GCs after PD-1 blockade with a significant increase in the expression of ICOS. When CD4$^+$ T cells and B cells from OVA-immunized mice were co-cultured with neutralizing anti-PD-1 Ab *in vitro,* PD-1 blockade recapitulated the up-regulation of ICOS expression on CD4$^+$ T cells with the activation of ERK signaling. Suppression of ERK activation not only reduced ICOS expression on CD4$^+$ T cells but also attenuated IgG production upon PD-1 blockade. Taken together, PD-1 blockade enhances humoral immunity. This process partially relies on more accumulation of CD4$^+$ T cells in GCs with the up-regulation of ICOS expression and the promotion of B cell terminal differentiation. The regulatory pattern of PD-1 blockade illustrated here provides a new mechanism of how immune checkpoint molecules regulating humoral immune responses.

1. Introduction

Being one of the key immune checkpoint molecules, programmed cell death protein 1 (PD-1) is extensively expressed on activated T cells including follicular T help cells (T_{FH}) and CD8$^+$ T cells [1,2]. It consists of a single extracellular IgV-like domain, a transmembrane domain, and an intracellular tail that contains an immunoreceptor tyrosine-based inhibition motif (ITIM) and an immunoreceptor tyrosine-based switch motif (ITSM) [3] exerting immune regulation on T cell functionality. PD-L1 (B7-H1) and PD-L2 (B7-DC) are two ligands of PD-1. They are expressed on germinal center (GC) B cells and dendritic cells [4]. More importantly, high PD-1 expression is a hallmark of CD8$^+$ T cell exhaustion in chronic infections and cancers [5]. With the expression of PD-1 ligands on certain tumor cells, its interaction with PD-1 leads to the apoptosis of activated T-cells [6]. Antibodies (Abs) targeting PD-1 or PD-L1 reverse the negative regulation mediated by PD-1 signaling and subsequently restore T cell functions [7]. PD-1/PD-L1 blockade reagents are of great success in clinical applications against multiple malignancies recently [8–10], validating the reversion of human T cell functionality as well. However, its role in regulating humoral immunity is not yet fully clear.

Several studies have suggested the roles of PD-1/PD-L signaling in regulating humoral immune responses with controversy. *In vivo* PD-1 blockade during simian immunodeficiency virus (SIV) infection increases envelope-specific Abs [11] while immunizing *B7-H1*$^{-/-}$ mice with helminth antigens results in significant elevation in Ag-specific immunoglobulin (Ig) responses with a profound increase in T_{FH} cells [12,13]. A recent publication has shown that PD-L1 expression on dendritic cells inhibits the differentiation of T_{FH} and T_{FR} cells as well [14]. PD-1 deficiency also leads to the dysregulated selection of IgA precursor cells in GCs of Peyer's patches and reshapes the gut microbiota [15]. However, other literatures reported the role of PD-1 signals in promoting humoral responses. For instance, the absence of PD-1 signaling was associated with lower GC B cell survival and less long-lived plasma cells [16]. Notably, T_{FH} cells have prominent expression of PD-1. T_{FH} cells at the T-B cell border are the main source of extrinsic

* Corresponding author at: Shanghai Institute of Immunology, Department of Immunology and Microbiology, Shanghai Jiao Tong University School of Medicine, 280 South Chongqing Road, Shanghai 200025, China.
E-mail address: ywang@sibs.ac.cn (Y. Wang).

https://doi.org/10.1016/j.intimp.2018.10.045
Received 26 September 2018; Received in revised form 26 October 2018; Accepted 31 October 2018
Available online 16 November 2018
1567-5769/

factors that promote GC formation, expansion and isotype switching [17–19]. Although the mode of PD-1 in regulating T_{FH} has been recently reported [20], its effects on GC responses and the consequence of Ab production as well as its mechanism have not yet been elucidated clearly.

Inducible T cell co-stimulator (ICOS) is a potent co-receptor that is inducibly expressed on activated T cells upon antigen stimulation [21]. It is also highly expressed on T_{FH} cells [22]. ICOS signaling is necessary for GC development and class switch through non-cognate T-B interaction [23]. Expression of ICOS on T_{FH} cells facilitates the recruitment and maintenance of T_{FH} cells in the follicles [24–26]. ICOS also performs an important function in mediating secondary humoral response to previously encountered T cell-dependent (TD) antigens [27].

In this study, we have investigated the effects of PD-1 blockade on humoral immunity by using TD antigen immunization. Our results showed that anti-PD-1 Ab treatment enhanced antibody production in ovalbumin (OVA)-immunized mice with increased percentages of GC B cells and plasma cells. More $CD4^+$ T cells were infiltrated in GC regions upon PD-1 blockade with higher expression of ICOS on $CD4^+$ T cells. *In vitro* assay demonstrated that up-regulation of ICOS on $CD4^+$ T cells was ERK dependent with the blockade of PD-1 signal. Our study thus provides the evidence on how PD-1/PD-L blockade regulating TD humoral response.

2. Materials and methods

2.1. Mice

BALB/c mice (female, 6–8 weeks) were purchased from SLAC laboratory animal center (Shanghai, China) and maintained under specific-pathogen-free (SPF) condition in the animal facility of Shanghai Jiao Tong University School of Medicine (Shanghai, China). To ameliorate any suffering of mice in experimental studies, mice were euthanized by CO_2 inhalation.

2.2. Immunizations and serum preparation

Mice were injected in foot pad with 100 μg of OVA (Sigma, St Louis, MO, USA) in 35 μL PBS mixed with 15 μL alum adjuvant (Thermo Fisher Scientific, Waltham, MA, USA) on day 0 and re-challenged with 100 μg OVA/alum on day 14. In the assay of affinity maturation, 100 μg NP45-CGG (Biosearch Technologies, Novato, CA, USA) in 100 μL PBS was mixed with equal volume of alum adjuvant, and was injected into the peritoneal cavity on days 0 and 14. For *in vivo* PD-1 blockade, mice were treated intra-peritoneally with 200 μg Rabbit anti-PD-1 polyclonal antibody (PcAb) (prepared by Youke Biotechnology Company, Shanghai, China) or control rabbit IgG on day 0, 2, and 4 after immunization with OVA or NP45-CGG. To exclude the interference of LPS in the experiment, the amount of endotoxin was measured by ToxinSensor™ Chromogenic LAL Endotoxin Assay Kit (GenScript, Nanjing, China). The antibodies used for *in vivo* assay contained endotoxin lower than 0.10–0.15 EU/mL (which was the limit for drugs by the FDA).

Blood was collected from the eye vein at different time points, kept at room temperature (RT) for 2 h and centrifuged at 5500 rpm for 10 min. The supernatants were collected and stored at −80 °C for ELISA assay.

2.3. Cell culture

Mice were injected in foot pad with OVA in alum adjuvant (five mice per group). One week later, mice were sacrificed. Spleens were collected and homogenized using a cell grinder. Single-cell suspensions were obtained by passing through 70-μm cell strainer (Falcon, Corning, NY, USA). Splenocytes were prepared through Ficoll-Hypaque density centrifugation. 2×10^5 splenocytes were stimulated with OVA (10 μg/mL) in 96-well plates (Corning, Corning, NY, USA) in a total volume of 200 μL RPMI 1640 culture medium containing 10% fetal bovine serum (FBS) (Millipore, Billerica, MA, USA), 50 μM 2-mercaptoethanol (Sigma), 100 units/mL penicillin (Gibco, Carlsbad, CA, USA), 100 μg/mL streptomycin (Gibco), 2 mM L-glutamine(Gibco) and Non-Essential Amino Acids Solution (Gibco) at 37 °C in a humidified atmosphere containing 5% CO_2. Cells were treated with 5 μg/mL anti-PD-1 (Clone J34, Armenian hamster; eBioscience, San Diego, CA, USA) or control isotype-matched IgG (Clone eBio299Arm, Armenian hamster; eBioscience) for 6 days. After the culture, cells were collected for flow cytometry and the supernatants were subjected to IgG and IgM detection. In some experiment, an ERK inhibitor FR180204 (Gene Operation, Ann Arbor, MI, USA) was added at a final concentration of 20 μM during the incubation.

2.4. ELISA

For determination of total IgG, IgG isotypes and IgM levels in the serum or culture supernatant, 96-well polystyrene plates (Corning) were coated with 2 μg/mL goat anti-mouse IgG(H + L) or 4 μg/mL goat anti-mouse IgM (SouthernBiotech, Birmingham, AL, USA) diluted in bicarbonate/carbonate coating buffer (15 mM Na_2CO_3 and 35 mM $NaHCO_3$, pH 9.6) and incubated at 4 °C overnight. After washing 3 times with PBST (PBS containing 0.05% Tween-20) (Sangon Biotech, Shanghai, China), the wells were blocked with 200 μL/well PBS containing 5% skimmed milk powder at RT for 2 h. Mouse serum or co-culture supernatants were serially diluted in PBST containing 3% skimmed milk powder. 100 μL diluted serum was added to the wells and the plates were incubated at RT for 2 h. After washing 3 times with PBST, the wells were incubated with horseradish peroxidase (HRP)-conjugated goat anti-mouse IgG(H + L), HRP-conjugated goat anti-mouse IgM (SouthernBiotech) or alkaline phosphatase (AP)-conjugated goat anti-mouse Ab for mouse IgG isotypes (Rockland, Gilbertsville, PA, USA) working solution (1:4000 diluted in PBST containing 3% skimmed milk powder, 100 μL/well), respectively at RT for 2 h. Tetramethylbenzidine (TMB) (BD Bioscience, San Diego, CA, USA) solution (for total IgG and IgM) or VISIGLO AP CHEMILUM SUBSTRATE (Sigma) solution (for IgG isotypes) (100 μL/well) was added, and the plates were incubated at RT in the dark for 15 min. The reaction was stopped by adding 1 M H_2SO_4 (50 μL/well) solution (for HRP) or 5 M NaOH (50 μL/well) solution (for AP). The absorbance at 450 nm (for TMB) or 405 nm (for VISIGLO AP CHEMILUM SUBSTRATE) was detected within 5 min by PowerWaveXS2 microplate spectrophotometer (BioTek, Burlington, VT, USA).

For measuring OVA specific antibodies, 96-well ELISA plates (Corning) were coated with 10 μg/mL (100 μL/well) OVA (Sigma) in coating buffer at 4 °C overnight. After washing 3 times with PBST (Sangon Biotech), the wells were blocked with 200 μL/well blocking buffer at RT for 2 h. 100 μL/well diluted serum was added to the wells for 2 h' incubation at RT. After washing 3 times with PBST (Sangon Biotech), HRP-conjugated goat anti-mouse IgG(H + L) (SBA) working solution was added in the well and incubated at RT for 2 h. *O*-Phenylenediamine (OPD) (YEASEN, Shanghai, China) solution (100 μL/well) was added and the plates were incubated at RT in the dark for 15 min. The reaction was stopped by adding 1 M H_2SO_4 (50 μL/well). The absorbance at 492 nm was detected within 5 min by PowerWaveXS2 microplate spectrophotometer (BioTek).

In affinity maturation assay, 10 μg/mL (100 μL/well) NP7-BSA (for high-affinity anti-NP Ab) (Biosearch Technologies) and NP30-BSA (for total anti-NP Ab) (Biosearch Technologies) in coating buffer were added in 96-well ELISA plates and incubated overnight at 4 °C. For detection, TMB (BD Bioscience) solution (100 μL/well) was added and the plates were incubated at RT in the dark. The absorbance at 650 nm was detected by PowerWaveXS2 microplate spectrophotometer (BioTek) without adding stop solution. The level of affinity maturation was calculated based on the ratio of OD_{650} of anti-NP7 Ab and anti-

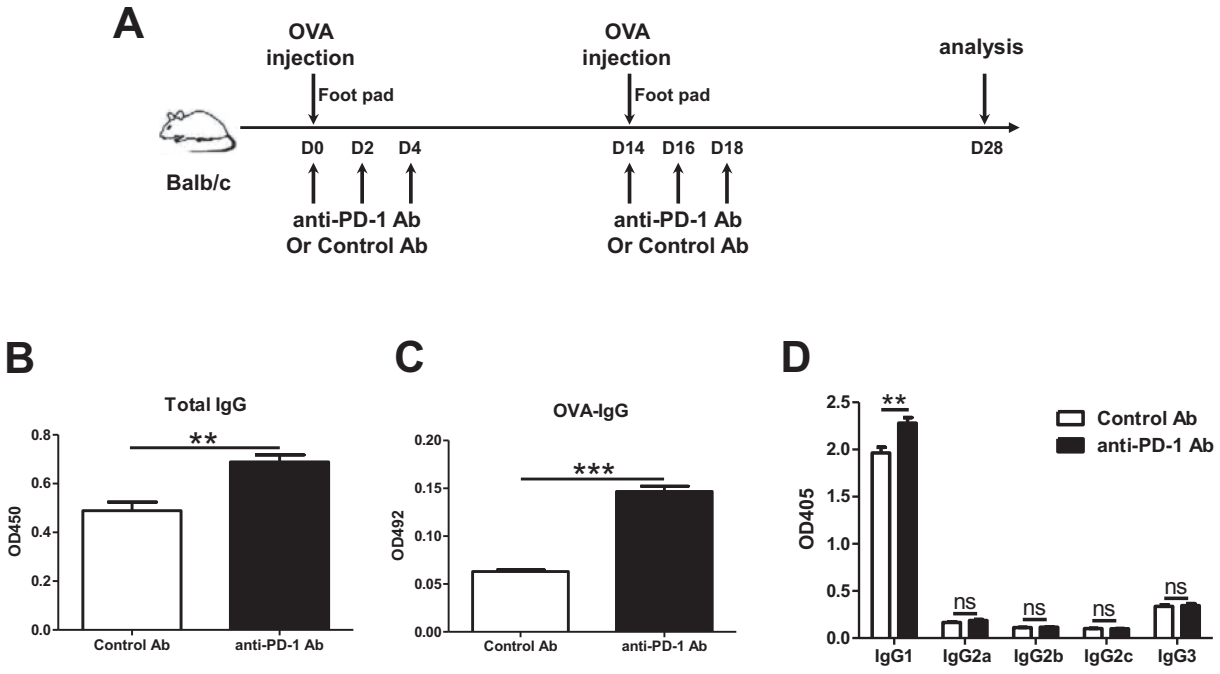

Fig. 1. PD-1 blockade *in vivo* enhances antibody production in OVA immunized mice.
(A) Flow Chart of the experiment procedure. BALB/c mice were vaccinated intra-peritoneally (i.p.) with 100 μg OVA in Alum on day 0 and treated with 200 μg anti-PD-1 Ab (i.p.) at days 0, 2, 4, 14, 16, and 18. Mice were boosted at days 14 and antibody levels measured at day 14 post-revaccination. (B-D) Levels of total IgG (B), OVA-specific IgG (C), and IgG subtypes (D) in the serum were measured by ELISA. Data were the representative of three independent experiments with at least 5 mice per group in each experiment. ns: not significant; **: $p < 0.01$, ***: $p < 0.001$.

NP30 Ab at an optimal time point.

2.5. Enzyme-linked Immunospot (ELISPOT) assay

OVA-specific antibody secreting cells (ASCs) were detected by ELISPOT kit (U-CyTech biosciences, Utrecht, Netherlands) according to manufacturer's instructions. Briefly, 96-well PVDF plates (Millipore) were coated with 10 μg/mL OVA overnight at 4 °C. The wells were blocked with PBS containing 1% BSA (Sangon Biotech) for 2 h at RT. 1×10^4 splenocytes or 1×10^6 cells from bone marrow in 200 μL culture medium were plated in each well. After 20 h of incubation at 37 °C, the plates were incubated with HRP-conjugated goat anti-mouse IgG(H + L) (SouthernBiotech) working solution (1:4000 dilution) at RT for 2 h. AEC substrate solution (eBioscience) was added in each well for 30 min in the dark at RT. Color development was stopped by thoroughly rinsing both sides of PVDF membrane with demineralized water. The plates were dried in the dark at RT. The spots were counted by ELISPOT BioReader-4000 (BIO-SYS GmbH, Karben, Germany). The numbers of OVA-specific ASC cells were calculated based on spot-forming units (SFUs) after deducting the background SFUs from the paired negative control.

2.6. Flow cytometry

For flow cytometry, cells were washed once with FACS buffer (1 × PBS supplemented with 2% FBS) and stained with antibodies against surface molecules including APC-Cy7-conjugated anti-CD19, Percp-cy5.5-conjugated anti-CD45R, Pacific Blue-conjugated anti-CD4, PE-conjugated anti-IgG1, APC-conjugated anti-CD54, PE-conjugated anti-CD279, APC-conjugated anti-CXCR5, PE-Cy7-conjugated anti-CXCR5 (all from BD Biosciences), Pacific Blue-conjugated anti-GL7, PE-conjugated anti-CD152 (Biolegend, San Diego, CA, USA), FITC-conjugated anti-Bcl6 (Santa Cruz Biotechnology, CA, USA) and APC-conjugated anti-CD278, Alexa Fluor 488-conjugated anti-CD95, Alexa Fluor 700-conjugated anti-CD38 (eBioscience) diluted in FACS buffer. Cells were stained at 4 °C for 30 min. Phospho-ERK protein was determined by using rabbit anti-mouse p-ERK1/2 (Thr202/Tyr204) (Cell Signaling Technology, Boston, MA, USA) as a primary antibody and Alexa Fluor 488-conjugated goat anti-rabbit IgG H&L antibody (Abcam, Cambridge, UK) as a secondary antibody. Intracellular staining assay were performed by using Foxp3/Transcription Factor Buffer Staining Set according to the manufacturer's instructions (eBioscience). Samples were collected on an LSR Fortessa (BD Biosciences) and data analysis was carried out with FlowJo 7.6 software (Tree Star, Ashland, OR, USA).

2.7. Immunofluorescence assay

Frozen sections of spleens were stained with the following Abs: Alexa Fluor 647-labeled anti-CD4 (Biolegend), FITC-labeled anti-B220 (BD Biosciences), rabbit anti-mouse Bcl6 (Abcam) and Alexa Fluor 568 conjugated Goat anti-rabbit IgG(H + L) secondary antibody (Thermo Fisher). DAPI (BD Biosciences) was used for nuclei staining at RT for 5 min before the observation. Stained sections were mounted with Fluoromount-G reagent (YEASEN) before the observation. Fluorescence signal was determined under a TCS SP8 confocal microscope (Leica, Solms, Germany).

2.8. Statistical analysis

Data were presented as means ± standard error of means (S.E.M). Statistical analyses were performed by using Graphpad Prism 5.0 software (Graphpad Prism, La Jolla, CA, USA). Statistic difference was determined *via* unpaired Student *t*-test for the data with Gaussian distribution or Mann-Whitney test for those with non-Gaussian distribution. Paired Student *t*-test was used when comparing antibody levels of supernatant. Unless stated, $p < 0.05$ was considered statistically significant.

3. Results

3.1. In vivo blockade of PD-1 enhances humoral responses in OVA immunized mice

To explore the effects of PD-1 blockade on humoral responses, we firstly determined the PD-1 expression on $CD4^+$ T cells upon TD antigen immunization. Consistent with the previous study [28], the expressions of PD-1 on $CD4^+$ T cells in the spleens were both elevated upon OVA (Supplemental Fig. 1A and B) or NP45-CGG (Supplemental Fig. 1C and D) immunization. Mice immunized with OVA were then intraperitoneally injected with rabbit anti-PD-1 PcAb or control rabbit IgG (Fig. 1A). The specificity of rabbit anti-PD-1 PcAb to PD-1 was verified by Western Blotting (Supplementary Fig. 2) and flow cytometry (Supplementary Fig. 3). It was found that total IgG and OVA-specific IgG levels in the serum of immunized mice increased significantly in anti-PD-1 Ab treated mice when compared to control mice (Fig. 1B and C). Notably, serum IgG1 was elevated more dramatically in anti-PD-1 Ab group than other IgG subtypes, such as IgG2a, IgG2b, IgG2c and IgG3 (Fig. 1D). Therefore, PD-1 blockade *in vivo* leads to the increased antibody production in OVA immunized mice.

3.2. PD-1 blockade has no significant effects on Ab affinity maturation

Affinity maturation is one of the key events during humoral immunity occurring in GCs. Whether PD-1/PD-L signal is engaged in this process is not yet reported. Therefore, a well-established protocol by using NP45-CGG immunization followed by determination of anti-NP7/anti-NP30 Ab ratio was adapted [29,30] (Fig. 2A). When NP45-CGG immunized mice were treated with anti-PD-1 PcAb or control rabbit IgG, total IgG levels increased significantly in anti-PD-1 Ab treated mice when compared to control mice both at the priming stage (Fig. 2B) and boosting stage (Fig. 2C). However, the ratio of anti-NP7 to anti-NP30 IgG was comparable between groups with or without anti-PD-1 blockade (Fig. 2D). These results thus illustrate that PD-1 blockade had no significant effects on Ab affinity maturation.

3.3. PD-1 blockade promotes B cell differentiation into plasma cells and memory B cells together with the expansion of GC B cells

GCs are the clusters containing rapidly dividing B cells to form secondary lymphoid tissues in response to TD antigens. Within GCs, somatic hypermutations at V regions of B cell receptors (BCR) facilitates the subsequent selection of high-affinity B cells and the generation of plasma cells producing high-affinity Ab and memory B cells, which is defined as the process of B cell terminal differentiation [31]. Since antibody production against TD antigens was enhanced with the blockade of PD-1 signals (Fig. 1), we further intended to clarify the effects of PD-1 blockade on B cell terminal differentiation. B cell subsets at different differentiation stages were determined in the spleens of OVA-immunized mice with or without anti-PD-1 Ab treatment (Fig. 1A). It was showed that the accumulation of $CD19^+B220^+CD95^+GL7^+$ GC B cells (Fig. 3A and B) and $CD19^+B220^+CD38^+IgG1^+$ memory B cells (Fig. 3C and D) in anti-PD-1 Ab treated mice were more dramatic than those without the treatment. Although $B220^-CD138^+$ plasma cells in the spleens were comparable between groups with or without PD-1 blockade (data not shown), OVA-specific IgG secreting cells in the spleens (Fig. 3E) and bone marrow (Fig. 3F), determined by ELISPOT assay, increased in anti-PD-1 treated mice, which was consistent with the elevated Ig levels in anti-PD-1 Ab treated mice in response to OVA immunization. These results demonstrate that blockade of PD-1/PD-L signal exaggerates GC responses and promotes B cell terminal differentiation in response to TD antigen.

3.4. Blocking PD-1 promotes the formation of GC and accumulation of T_{FH} cells in the spleens of immunized mice

The interaction between $CD4^+$ T_{FH} cells and B cells is critical for GC formation. In order to provide help to B cells, extra-follicular activated T cells are supposed to migrate to B-cell zones in the follicles of GCs with the downregulation of C—C chemokine receptor type 7 (CCR7), and concomitant upregulation of C-X-C chemokine receptor type 5 (CXCR5), one of the key signatures of T_{FH} cells in GCs. The shifted expression profile of chemokine receptors on activated T cells facilitates cell migration along with the gradient of its ligand chemokine (C-X-C motif) ligand 13 (CXCL13) thereafter [32]. Herein, we detected the effects of PD-1 blockade on the formation of GCs at day 14 post-re-vaccination. It was apparent that PD-1 blockade induced a significant increase in the GC number (Fig. 4A-C). Consistent with these findings, the percentage of T_{FH} ($CXCR5^+Bcl6^+CD4^+$) increased significantly in anti-PD-1 treated OVA immunized mice as well (Fig. 4D and E). Taken together, the results described above indicated that PD-1 blockade after immunization leads to the accumulation of T_{FH} cells, which is feasible to provide more extrinsic help for GC formation and B cell terminal differentiation.

3.5. ICOS is upregulated on $CD4^+$ T cells in immunized mice upon anti-PD-1 treatment

To investigate the factors that might be responsible for the accumulation of $CD4^+$ T cells in GCs upon PD-1 blockade, we analyzed the phenotypes of $CD4^+$ T cells related to cell adhesion and migration. It was shown that the expression levels of ICAM-1 (Fig. 5A) and CTLA-4 (Fig. 5B) were comparable between anti-PD-1 Ab treated mice and control mice. Notably, the expression levels of ICOS (Fig. 5C) and CXCR5 (Fig. 5D) on $CD4^+$ T cells increased significantly in mice treated with anti-PD-1 Ab when compared to control mice. ICOS has been demonstrated to directly control follicular recruitment of activated $CD4^+$ T cells and the residence of T cells at the T-B border *in vivo* [33]. Therefore, in our study up-regulation of ICOS on $CD4^+$ T cells is observed upon PD-1 blockade, which is beneficial for T cells to migrate to the follicles and provide more efficient help for B cell terminal differentiation.

3.6. The up-regulation of ICOS on $CD4^+$ T cells upon PD-1 blockade is ERK dependent

To determine the mechanisms of ICOS upregulation on $CD4^+$ T cells upon PD-1 blockade, splenocytes from OVA immunized mice were stimulated with OVA *in vitro* and anti-PD-1 Ab were added simultaneously (Fig. 6A). The expression level of ICOS on $CD4^+$ T cells and the IgG/IgM levels in the culture supernatants were detected 6 days later. Results from ELISA analysis showed that the IgG and IgM levels increased in the culture supernatants from the group treated with anti-PD-1 Ab as compared with control group (Fig. 6B). Both the percentage and the mean fluorescence intensity (MFI) of ICOS on $CD4^+$ T cells increased significantly in anti-PD-1 Ab treated group as well (Fig. 6C-E). More interestingly, there was a positive correlation between the IgG/IgM levels in the supernatants and the expression levels of ICOS on $CD4^+$ T cells (Fig. 6F). These results are consistent with the data we obtained from *in vivo* assay that blocking PD-1 promotes the production of antibody and the expression of ICOS on $CD4^+$ T cells.

ERK activation is reported to be involved in the induction of ICOS after T cell activation [34]. We simultaneously determined the phospho-ERK (p-ERK) level in $ICOS^+CD4^+$ T cells after *in vitro* blockade. It was found that p-ERK level in $ICOS^+CD4^+$ T cells was significantly elevated in anti-PD-1 treated group when compared to control group (Fig. 7A). This result suggested that ERK signaling might be involved in the regulation of ICOS expression on $CD4^+$ T cells after blocking PD-1 signal. To verify the speculation, we further stimulated

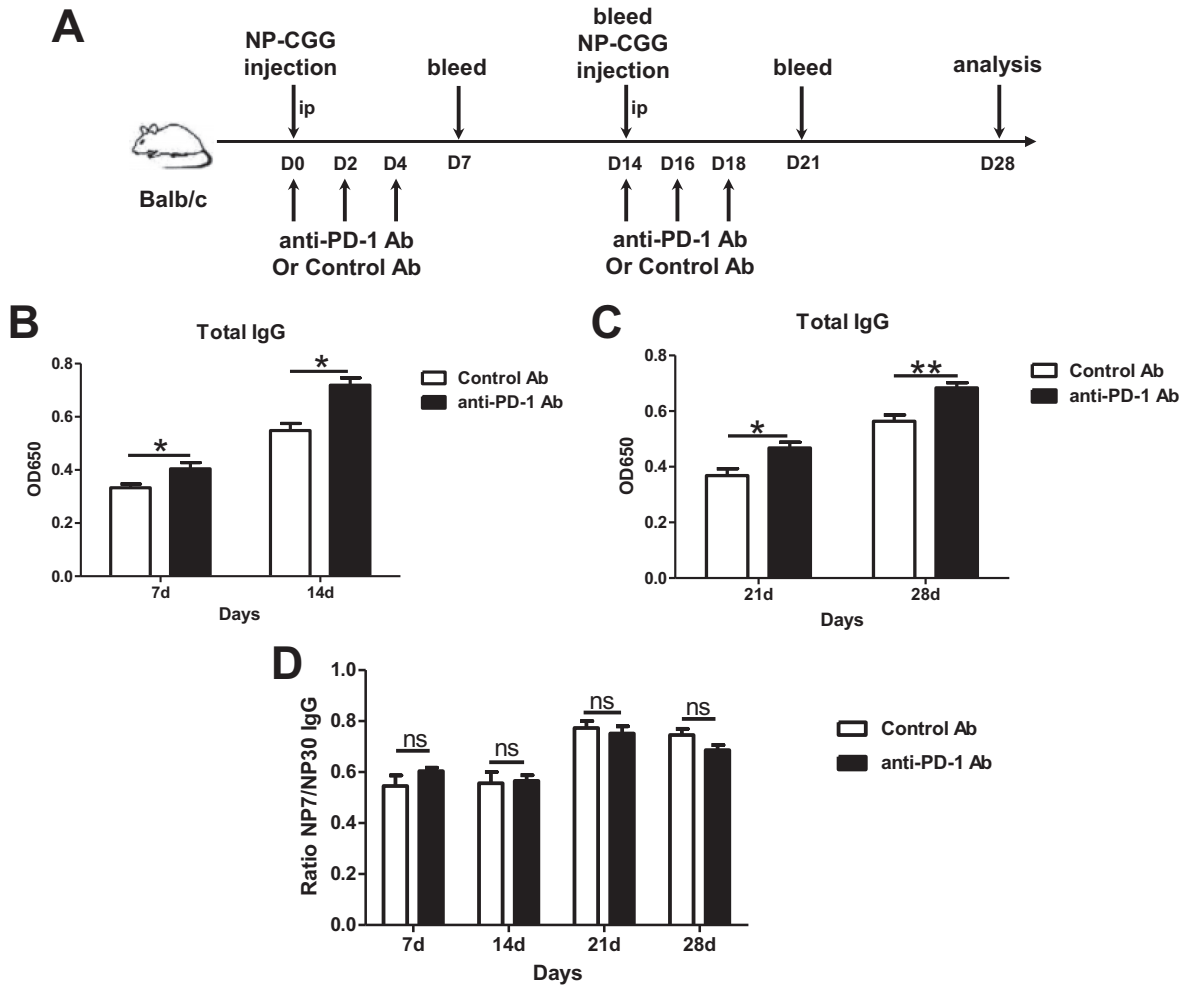

Fig. 2. PD-1 blockade has no significant effects on antibody affinity maturation.
(A) Flow Chart of the experiment procedure. BALB/c mice were primed i.p. with 100 μg NP45-CGG in Alum on day 0, and boosted at days 14. 200 μg anti-PD-1 Ab was injected i.p. at days 0, 2, 4, 14, 16, and 18. Ab levels against NP7-BSA and NP30-BSA were measured at day 14 post-revaccination. (B) Total IgG levels at day 7 (early priming stage) and day 14 (late priming stage). (C) Total IgG levels at day 21 and day 28 (both at boosting stages). (D) Ratios of anti-NP7-BSA Ab (high affinity NP-specific Ab) and anti-NP30-BSA antibody (total NP-specific Ab) at day 7, day 14, day 21, and day 28. Data were the representative of two independent experiments with at least 5 mice per group in each experiment. ns: not significant; *: $p < 0.05$, **: $p < 0.01$.

splenocytes from OVA immunized mice with OVA and treated them with anti-PD-1 Ab with or without ERK inhibitor FR180204 (Fig. 7B). The expression levels of ICOS on $CD4^+$ T cells were compared. It was shown that ICOS expression level on $CD4^+$ T cells reduced significantly when FR180204 was added compared with those with vehicle treatment (Fig. 7C and D). What is more, the IgG and IgM levels reduced in parallel in the supernatants from the group treated with FR180204 (Fig. 7E). Therefore the up-regulation of ICOS on $CD4^+$ T cells upon PD-1 blockade is ERK dependent.

4. Discussion

PD-1/PD-L signaling is one of the key costimulatory pathways that balances the activation and inhibition on T cell functionality both in the defense against microbes and the maintenance of self-tolerance and homeostasis [35]. Investigations on the biological significance of PD-1 overexpression on T cells has originally revealed its engagement in the exhaustion of $CD8^+$ T cells [36,37]. Further investigations demonstrates its roles in the maintenance of T cell anergy in chronic viral infections and cancers [38,39]. However, the regulatory roles of PD-1 on $CD4^+$ T cells are still not fully clarified. Previous study has reported that disruption of PD-1/PD-L signaling resulted in autoimmunity in BALB/C and B6 mice [40,41], suggesting a role of PD-1/PD-L signaling in the maintenance of immune tolerance. Other studies, on the contrary, have reported the attenuated humoral responses when interactions between PD-1 and its ligands were interrupted [16,42]. In our study, we observed that the treatment of anti-PD-1 blocking antibody promoted antibody production in OVA immunized mice with no effects on affinity maturation. We further investigated the influence of PD-1 blockade on B cell terminal differentiation owing to the observation of enhanced antibody production. Indeed, PD-1 blockade in OVA immunized mice was associated with more GC B cells and memory B cells in the spleens as well as more antibody secreting cells in the spleens and bone marrow. Thus, PD-1/PD-L signaling appears to be involved in the modulation of B cell terminal differentiation when encountering foreign antigens.

It is well accepted that B cell terminal differentiation occurs in GCs, a lymphoid structures formed during humoral responses to TD antigen. In GCs, full activation and differentiation of B cells rely on the interaction with T_{FH} cells as well as follicular dendritic cells (FDCs). While FDCs are responsible for enriching and presenting Ags to B cells, T_{FH} cells are more involved in providing non-specific stimulatory signals for B cell activation and differentiation. Sustained T-B interactions in GCs are indispensable for Ig class switching, maintenance of GC reaction, and selection of high-affinity B cell clones [43,44]. The roles of PD-1 in GCs are diverse. Several types of immune cells in GCs express high level

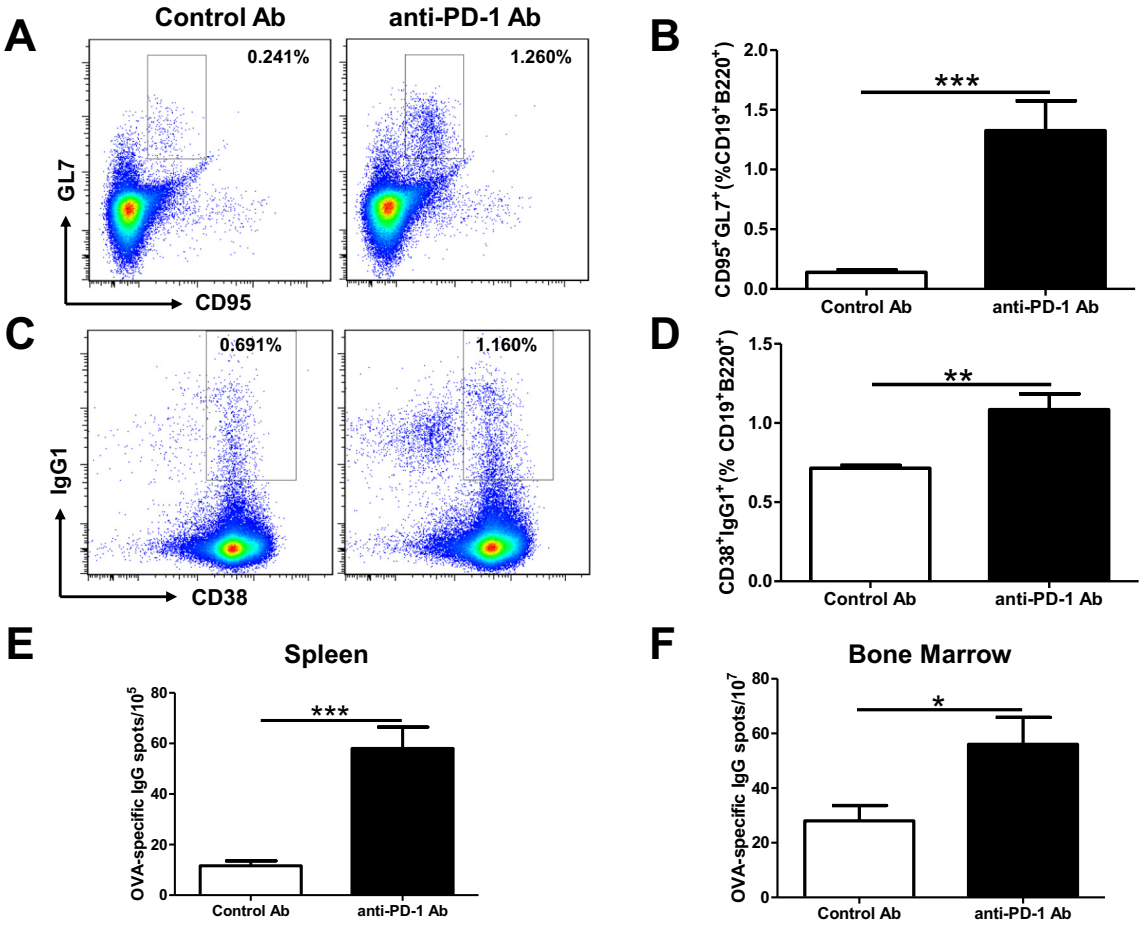

Fig. 3. PD-1 blockade *in vivo* promotes B cell terminal differentiation.
OVA-immunized mice were sacrificed at day 14 post-revaccination. (A) $CD19^+B220^+CD95^+GL7^+$ GC B cells in the spleens of mice with or without anti-PD-1 treatment. (B) Comparison of the percentages of GC B cells in the spleens of OVA-immunized mice with anti-PD-1 or control Abs treatment. (C) $CD19^+B220^+CD38^+IgG1^+$ memory B cells in the spleens of OVA-immunized mice with or without anti-PD-1 treatment. (D) Comparison of the percentages of memory B cells in the spleens of OVA-immunized mice with or without anti-PD-1 treatment. (E, F) Statistics of OVA-specific IgG secreting cells in spleens (E) and bone marrow (F), respectively. Data were pooled from three independent experiments with at least 5 mice per group in each experiment. *: $p < 0.05$, **: $p < 0.01$, ***: $p < 0.001$.

of PD-1. For instance, PD-1 is one of the key surface signatures of T_{FH} cells. The role of PD-1 blockade on T_{FH} cells have been reported previously [16]. $CD4^+CXCR5^+FOXP3^+$ follicular regulatory T cells (T_{FR}) also express high levels of PD-1 [45]. Deficiency of PD-1 in T_{FR} cells augments the generation of T_{FH} cells and subsequence antibody responses. PD-1 expression on B cells is not well understood. Some studies suggest that PD-1 plays a crucial role in malignant B-cell development [46]. However, the direct effect on B cells after anti-PD-1 blockade needs to be investigated in the future investigation. In addition, there reported the existence of $PD\text{-}L1^{hi}$ regulatory B cells in GCs [47]. They could suppress humoral immunity through attenuating T cell activation. In our study we have demonstrated that more $CD4^+$ T cells were infiltrated in GCs with the upregulation of ICOS and CXCR5 on $CD4^+$ T cells upon PD-1 blockade. Therefore, the effects of PD-1 blockade on antibody production in our *in vivo* study might reflect the outcome of comprehensive interaction between different types of immune cells in GCs. More likely, not only more accumulation of $CD4^+$ T cells, stronger humoral immunity upon PD-1 blockade might also be due to the interruption between T_{FH} and $PD\text{-}L1^{hi}$ regulatory B cells or T_{FH} and T_{FR} cells, which in turn augments the activation and function of T_{FH} cells in GCs. In fact, the observation of more infiltration of $CD4^+$ T cells in GCs upon PD-1 blockade, to some extent, is consistent with the reports by Qi' group that PD-1/PD-L1 signal is involved in positioning $CD4^+$ T_{FH} cells into GCs [20].

It is well accepted that both CXCR5 and ICOS favor the migration of activated T cells into B cell follicle [48]. CXCR5 is the ligand for CXCL13. Higher expression of CXCR5 on T_{FH} cells promotes the migration and position of T_{FH} cells into GCs where CXCL13 is high [48]. The roles of ICOS on $CD4^+$ T cells in GCs are more complex. In Xu's recent publication [33], it is proved that ICOS directly controls follicular recruitment of activated T-helper cells in mice. Dynamic imaging assay reveals the engagement of ICOS in driving coordinated pseudopod formation and promoting the position of T cell at the border between T-cell zone and B-cell follicle *in vivo*. In addition, ICOS is also involved in positive selection and affinity maturation in GCs in a feed-forward manner [25]. In our study, we observed that the presence of more $CD4^+$ T cells in GC regions was associated with the increased expression levels of ICOS and CXCR5 on $CD4^+$ T cells upon PD-1 blockade. We thus propose that PD-1 signaling might be engaged in the regulation of ICOS and CXCR5 expression on $CD4^+$ T cells.

To explore the mechanisms of PD-1 regulation on ICOS expression in $CD4^+$ T cells, an *in vitro* PD-1 blockade assay was adapted to recapitulate T-B interaction in GCs. Splenocytes from OVA immunized mice were stimulated with OVA *in vitro* and PD-1 blockade was performed simultaneously. Consistent with *in vivo* study, PD-1 blockade *in vitro* also resulted in enhanced production of IgG, which is positively correlated with the expression levels of ICOS on $CD4^+$ T cells. Additionally, the elevated level of p-ERK on $ICOS^+CD4^+$ T cells was

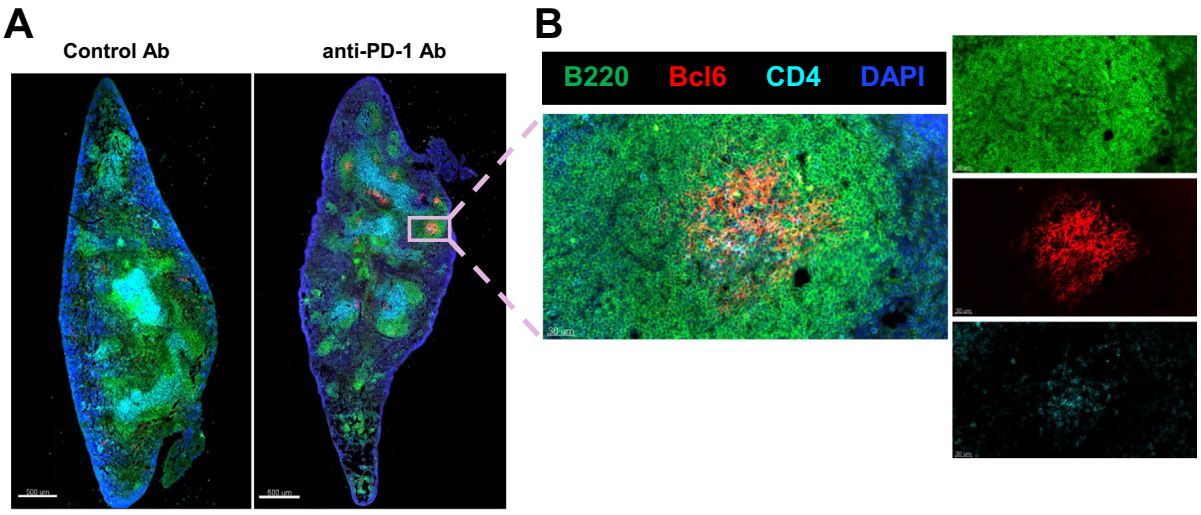

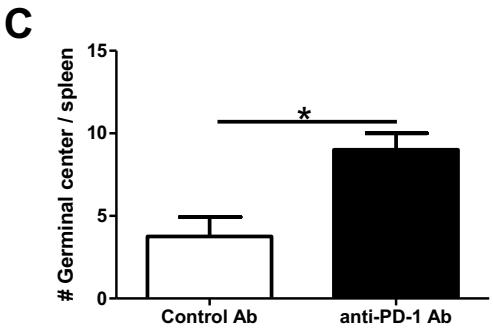

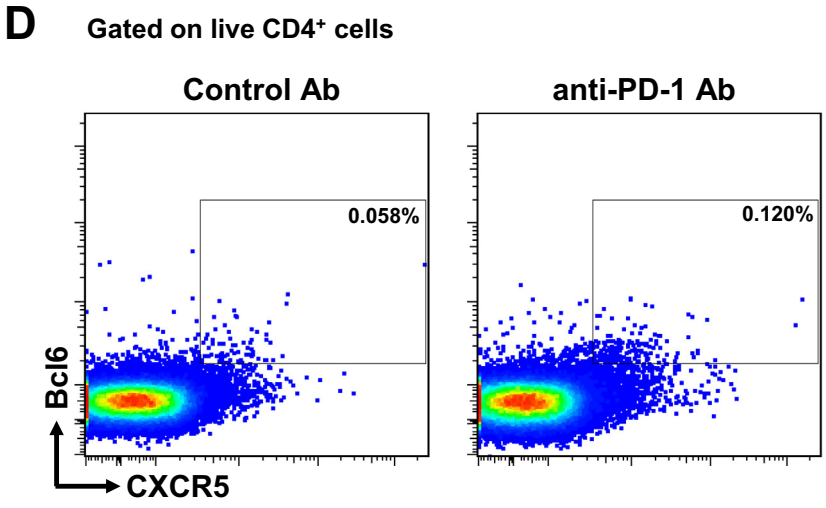

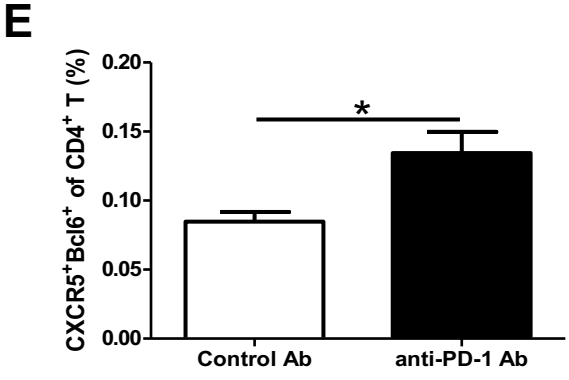

(caption on next page)

Fig. 4. Increased GC number and the accumulation of T_{FH} cells in the spleens upon anti-PD-1 treatment.
OVA-immunized mice were sacrificed at day 14 post-revaccination. Spleens were collected and frozen in OCT embedding medium. Frozen sections were stained by immunofluorescent antibodies, and analyzed by confocal microscopy. (A) Representative images from anti-PD-1 Ab or control Ab treated immunized mice. Scale bars: 500 μm (B) Magnification of a representative GC. $B220^+$ B cells were shown in green. $CD4^+$ cells were shown in cyan. $Bcl6^+$ GC cells were shown in red and cell nucleus were shown in blue. Data were pooled from two independent experiments. Scale bars: 30 μm. (C) Statistics of GCs per spleen section. (D) $CXCR5^+Bcl6^+CD4^+$ T_{FH} cells in the spleens of mice with anti-PD-1 or control Abs treatment. (E) Comparison of the percentages of T_{FH} cells in the spleens of OVA-immunized mice with anti-PD-1 or control Abs treatment. Data were pooled from two independent experiments with 5 mice per experiment. *: $p < 0.05$. (For interpretation of the references to color in this figure legend, the reader is referred to the web version of this article.)

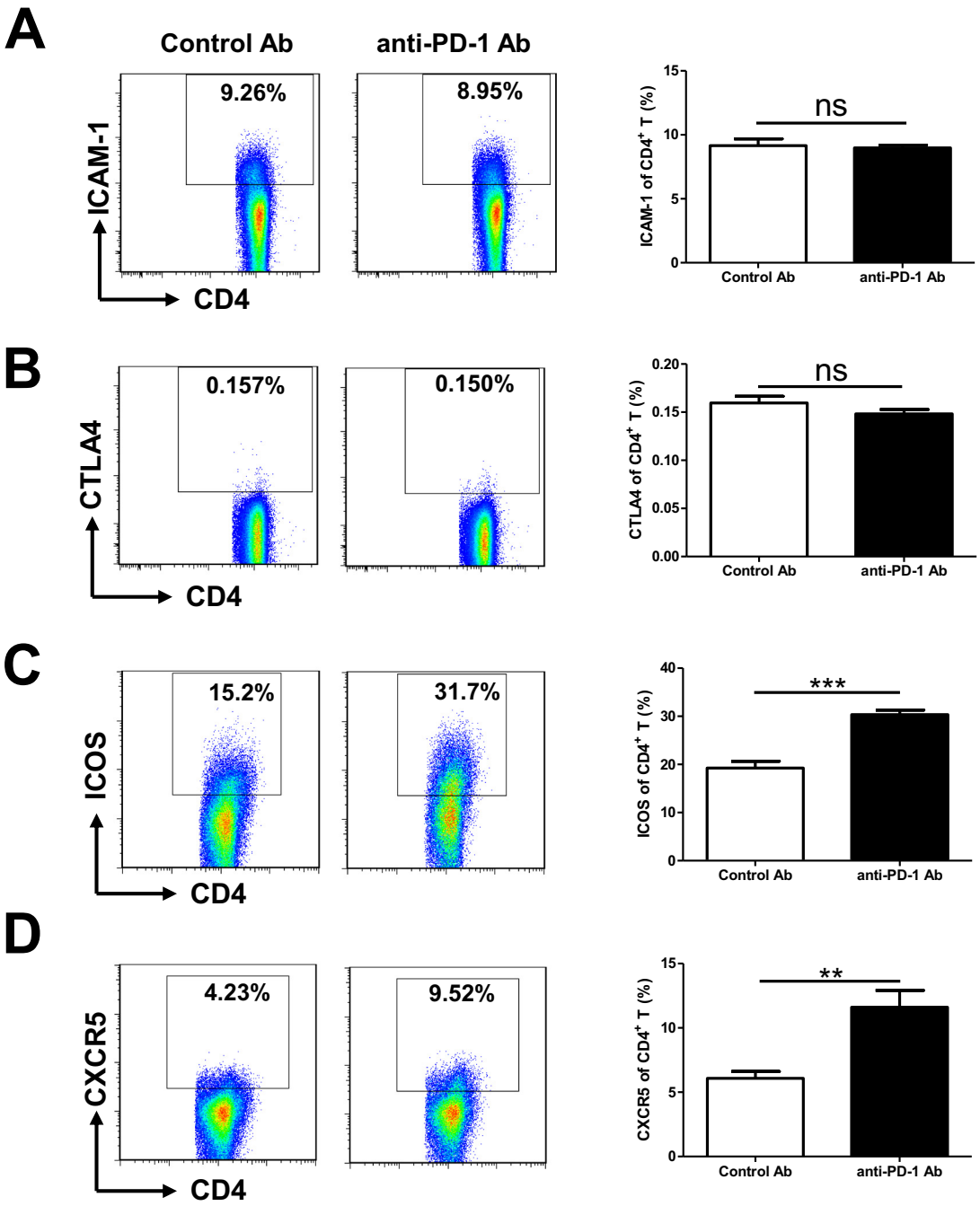

Fig. 5. Increased ICOS and CXCR5 expression on $CD4^+$ T cells after PD-1 blockade *in vivo*.
Expression of ICAM-1 (A), CTLA4 (B), ICOS (C) and CXCR5 (D) on $CD4^+$ T cells in the spleens from OVA-immunized mice with or without anti-PD-1 Ab treatment were determined by flow cytometry. Data were pooled from three independent experiments with 5 mice per group in each experiment. ns: not significant; **: $p < 0.01$, ***: $p < 0.001$.

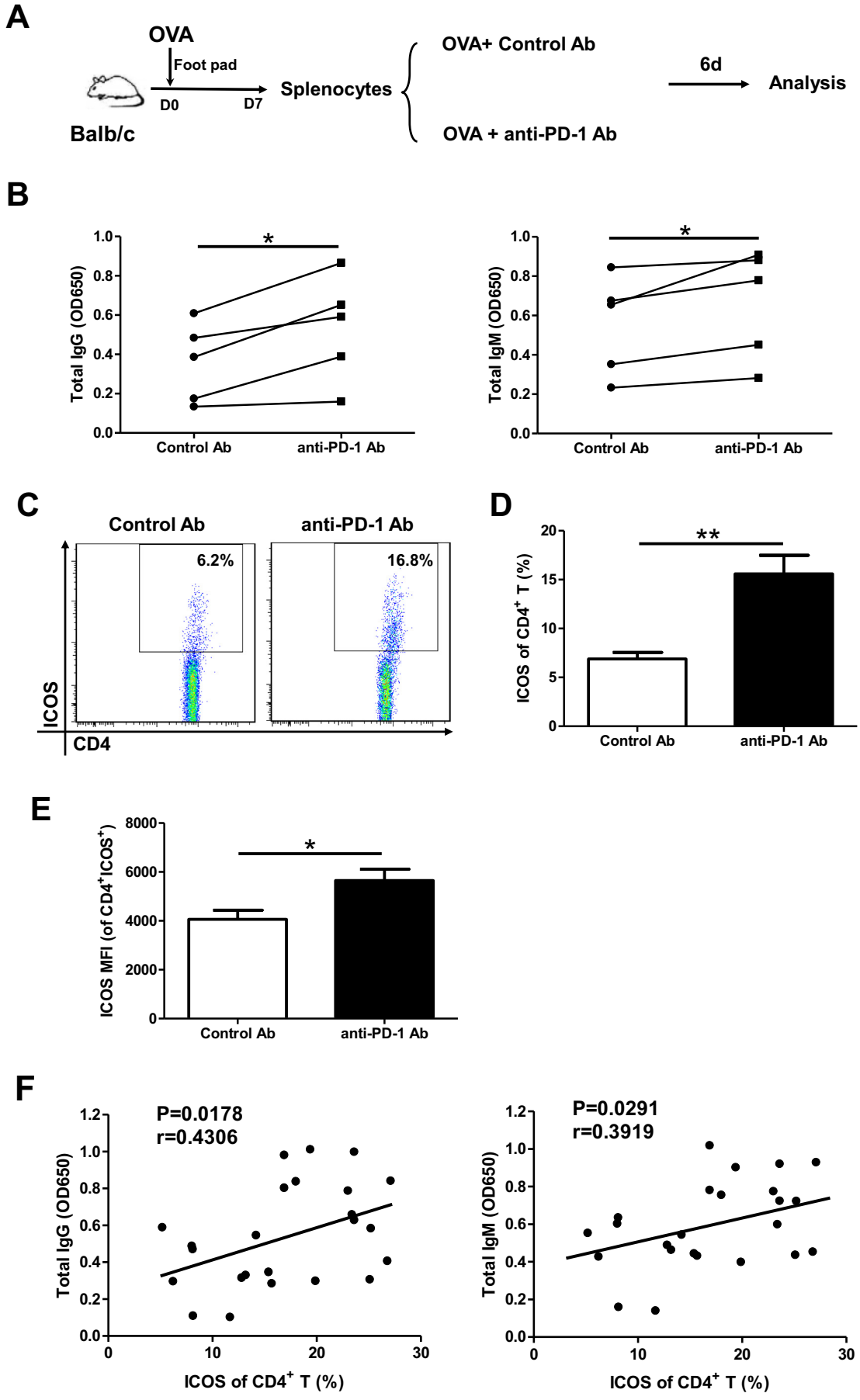

(caption on next page)

Fig. 6. PD-1 blockade *in vitro* recapitulates the upregulation of ICOS on $CD4^+$ T cells and the elevation of IgG/IgM upon PD-1 blockade.
(A) Flow chart of experimental procedure. Splenocytes were collected from OVA-immunized mice at day 7, and stimulated with OVA (10 μg/ml) and IgG isotype (control) or anti-PD-1 Ab. Cells and supernatants were collected and analyzed 6 days later. (B) Total IgG and IgM levels in the supernatants determined by ELISA. (C) Expression of ICOS on $CD4^+$ T cells. (D) Statistics of the percentages of $ICOS^+CD4^+$ T cells after the coculture. (E) Statistics of ICOS MFI in $CD4^+ICOS^+$ T cells. Data were pooled from three independent experiments. (F) Correlation analysis between ICOS expression on $CD4^+$ T cells and total IgG or IgM in the supernatants. The correlation coefficient *r* and the *P* value were calculated using the Spearman rank test. *: $p < 0.05$, **: $p < 0.01$.

detectable in anti-PD-1 Ab treated group, which could be attenuated by an ERK inhibitor. Our results presented here provide the clues that PD-1 signaling exerts inhibition on ERK activation in $CD4^+$ T cells, which in turn suppress ICOS expression on $CD4^+$ T cells. Molecular mechanisms concerning cross-talk between PD-1 and ERK signal pathways need to be further investigated.

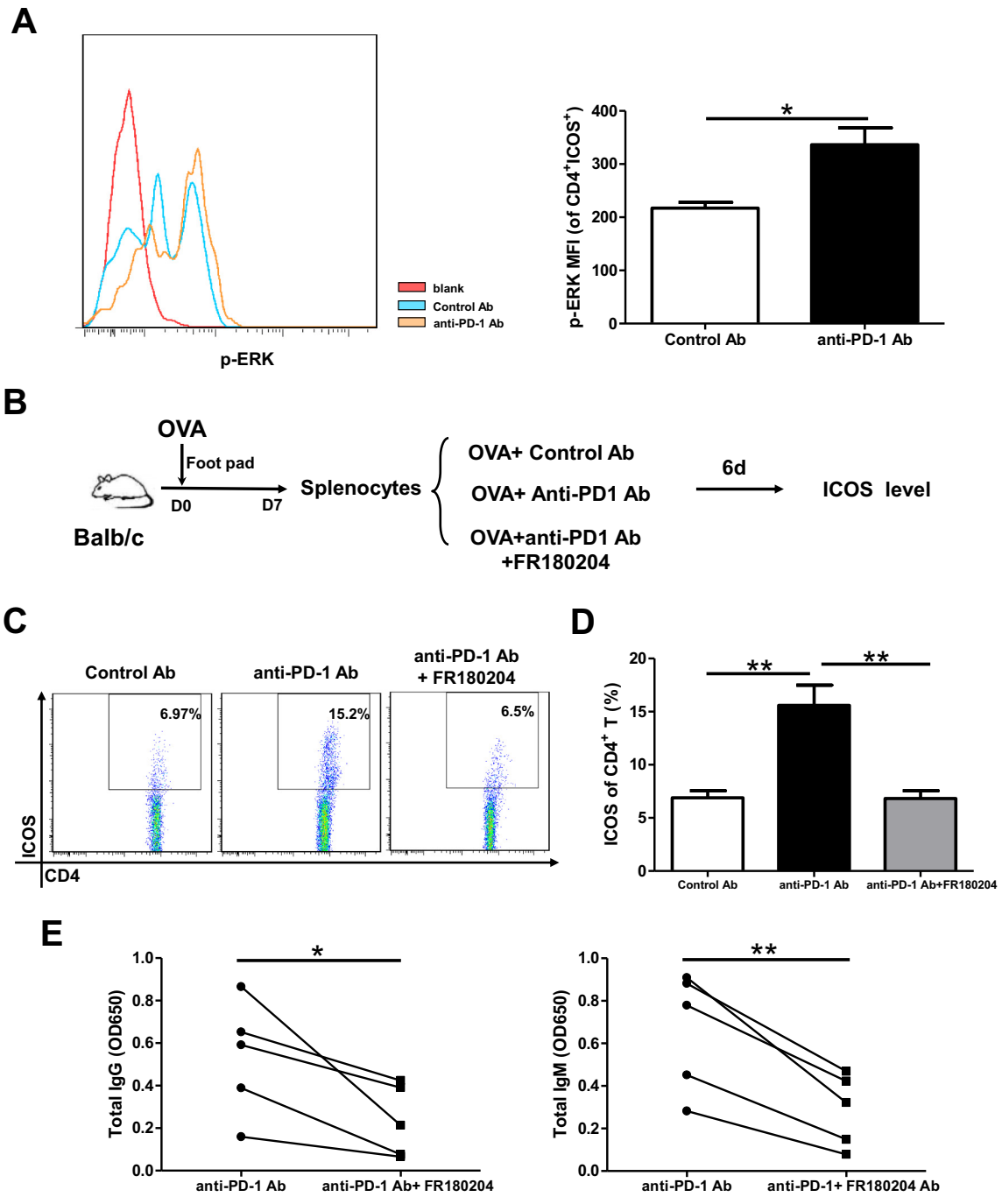

Fig. 7. The up-regulation of ICOS on $CD4^+$ T cells upon PD-1 blockade is ERK dependent.
(A) Flow cytometry (left) and MFI (right) analysis of p-ERK level in $ICOS^+CD4^+$ T cells from *in vitro* stimulation assay. (B) Flow chart of *in vitro* stimulation assay for ERK inhibition. (C) Comparison of ICOS expression on $CD4^+$ T cells from three groups of splenocytes accordingly. (D) Statistics of the percentage of $ICOS^+CD4^+$ T cells. (E) Total IgG and IgM levels in the supernatants. Data were pooled from three independent experiments. *: $p < 0.05$, **: $p < 0.01$.

5. Conclusion

In summary, we have herein proved that PD-1 blockade induced stronger humoral immunity, which is associated with the accumulation of $CD4^+$ T cells in GCs. This is partially due to the up-regulation of ICOS expression on $CD4^+$ T cells that favor the migration and position of $CD4^+$ T cells in GCs. The regulatory mode of PD-1 blockade illustrated here provides a new mechanism of how immune checkpoint molecules on T cells regulating humoral immune responses.

Ethical standards

The animal study was approved by the Scientific Investigation Board of Shanghai Jiao Tong University School of Medicine.

Funding

This study was supported by the grants from the National Key R&D Program of China (2016YFC1303300), the National Science Foundation of China (31370884), Clinical Research Plan of SHDC (16CR3005A) and Shanghai Academic Research Leader Project (2018XD1403300).

Acknowledgments

We appreciated Dr. Chuan-xin Huang, Dr. Fu-bin Li and Prof Bing Su for their kind suggestions and help on this study. We also thanked Wenwen Liu and Xujiao Feng (Shanghai Institute of Immunology, Institute of Medical Sciences, Shanghai Jiao Tong University School of Medicine) for their assistance in flow cytometry, and Prof. Hao Shen from University of Pennsylvania for the advice on data interpretation.

Conflict of interest

The authors declare that they have no conflict of interest.

Appendix A. Supplementary data

Supplementary data to this article can be found online at https://doi.org/10.1016/j.intimp.2018.10.045.

References

[1] D.L. Barber, E.J. Wherry, D. Masopust, B. Zhu, J.P. Allison, A.H. Sharpe, G.J. Freeman, R. Ahmed, Restoring function in exhausted CD8 T cells during chronic viral infection, Nature 439 (7077) (2006) 682–687.
[2] N.M. Haynes, C.D. Allen, R. Lesley, K.M. Ansel, N. Killeen, J.G. Cyster, Role of CXCR5 and CCR7 in follicular Th cell positioning and appearance of a programmed cell death gene-1high germinal center-associated subpopulation, J. Immunol. 179 (8) (2007) 5099–5108.
[3] X. Zhang, J.C. Schwartz, X. Guo, S. Bhatia, E. Cao, M. Lorenz, M. Cammer, L. Chen, Z.Y. Zhang, M.A. Edidin, S.G. Nathenson, S.C. Almo, Structural and functional analysis of the costimulatory receptor programmed death-1, Immunity 20 (3) (2004) 337–347.
[4] T. Yamazaki, H. Akiba, H. Iwai, H. Matsuda, M. Aoki, Y. Tanno, T. Shin, H. Tsuchiya, D.M. Pardoll, K. Okumura, M. Azuma, H. Yagita, Expression of programmed death 1 ligands by murine T cells and APC, J. Immunol. 169 (10) (2002) 5538–5545.
[5] E.J. Wherry, M. Kurachi, Molecular and cellular insights into T cell exhaustion, Nat. Rev. Immunol. 15 (8) (2015) 486–499.
[6] J.R. Brahmer, C.G. Drake, I. Wollner, J.D. Powderly, J. Picus, W.H. Sharfman, E. Stankevich, A. Pons, T.M. Salay, T.L. McMiller, M.M. Gilson, C. Wang, M. Selby, J.M. Taube, R. Anders, L. Chen, A.J. Korman, D.M. Pardoll, I. Lowy, S.L. Topalian, Phase I study of single-agent anti-programmed death-1 (MDX-1106) in refractory solid tumors: safety, clinical activity, pharmacodynamics, and immunologic correlates, J. Clin. Oncol. Off. J. Am. Soc. Clin. Oncol. 28 (19) (2010) 3167–3175.
[7] P.S. Kim, R. Ahmed, Features of responding T cells in cancer and chronic infection, Curr. Opin. Immunol. 22 (2) (2010) 223–230.
[8] Z. Guo, H. Wang, F. Meng, J. Li, S. Zhang, Combined Trabectedin and anti-PD1 antibody produces a synergistic antitumor effect in a murine model of ovarian cancer, J. Transl. Med. 13 (1) (2015).
[9] P. Armand, A. Nagler, E.A. Weller, S.M. Devine, D.E. Avigan, Y.B. Chen, M.S. Kaminski, H.K. Holland, J.N. Winter, J.R. Mason, J.W. Fay, D.A. Rizzieri, C.M. Hosing, E.D. Ball, J.P. Uberti, H.M. Lazarus, M.Y. Mapara, S.A. Gregory, J.M. Timmerman, D. Andorsky, R. Or, E.K. Waller, R. Rotem-Yehudar, L.I. Gordon, Disabling immune tolerance by programmed Death-1 blockade with pidilizumab after autologous hematopoietic stem-cell transplantation for diffuse large B-cell lymphoma: results of an international phase II trial, J. Clin. Oncol. 31 (33) (2013) 4199–4206.
[10] J.R. Westin, F. Chu, M. Zhang, L.E. Fayad, L.W. Kwak, N. Fowler, J. Romaguera, F. Hagemeister, M. Fanale, F. Samaniego, L. Feng, V. Baladandayuthapani, Z. Wang, W. Ma, Y. Gao, M. Wallace, L.M. Vence, L. Radvanyi, T. Muzzafar, R. Rotem-Yehudar, R.E. Davis, S.S. Neelapu, Safety and activity of PD1 blockade by pidilizumab in combination with rituximab in patients with relapsed follicular lymphoma: a single group, open-label, phase 2 trial, Lancet Oncol. 15 (1) (2014) 69–77.
[11] V. Velu, K. Titanji, B. Zhu, S. Husain, A. Pladevega, L. Lai, T.H. Vanderford, L. Chennareddi, G. Silvestri, G.J. Freeman, R. Ahmed, R.R. Amara, Enhancing SIV-specific immunity in vivo by PD-1 blockade, Nature 458 (7235) (2009) 206–210.
[12] E. Hams, M.J. McCarron, S. Amu, H. Yagita, M. Azuma, L. Chen, P.G. Fallon, Blockade of B7-H1 (programmed death ligand 1) enhances humoral immunity by positively regulating the generation of T follicular helper cells, J. Immunol. 186 (10) (2011) 5648–5655.
[13] V. Velu, K. Titanji, B. Zhu, S. Husain, A. Pladevega, L. Lai, T.H. Vanderford, L. Chennareddi, G. Silvestri, G.J. Freeman, R. Ahmed, R.R. Amara, Enhancing SIV-specific immunity in vivo by PD-1 blockade, Nature 458 (7235) (2008) 206–210.
[14] P.T. Sage, F.A. Schildberg, R.A. Sobel, V.K. Kuchroo, G.J. Freeman, A.H. Sharpe, Dendritic cell PD-L1 limits autoimmunity and follicular T cell differentiation and function, J. Immunol. 200 (8) (2018) 2592–2602.
[15] M. Maruya, S. Kawamoto, L.M. Kato, S. Fagarasan, Impaired selection of IgA and intestinal dysbiosis associated with PD-1-deficiency, Gut Microbes 4 (2) (2013) 165–171.
[16] K.L. Good-Jacobson, C.G. Szumilas, L. Chen, A.H. Sharpe, M.M. Tomayko, M.J. Shlomchik, PD-1 regulates germinal center B cell survival and the formation and affinity of long-lived plasma cells, Nat. Immunol. 11 (6) (2010) 535–542.
[17] C.D. Allen, T. Okada, H.L. Tang, J.G. Cyster, Imaging of germinal center selection events during affinity maturation, Science 315 (5811) (2007) 528–531.
[18] K.M. Toellner, A. Gulbranson-Judge, D.R. Taylor, D.M. Sze, I.C. MacLennan, Immunoglobulin switch transcript production in vivo related to the site and time of antigen-specific B cell activation, J. Exp. Med. 183 (5) (1996) 2303–2312.
[19] Y.J. Liu, J. Zhang, P.J. Lane, E.Y. Chan, I.C. MacLennan, Sites of specific B cell activation in primary and secondary responses to T cell-dependent and T cell-independent antigens, Eur. J. Immunol. 21 (12) (1991) 2951–2962.
[20] J. Shi, S. Hou, Q. Fang, X. Liu, X. Liu, H. Qi, PD-1 controls follicular T helper cell positioning and function, Immunity 49 (2) (2018) 264–274.
[21] A. Hutloff, A.M. Dittrich, K.C. Beier, B. Eljaschewitsch, R. Kraft, I. Anagnostopoulos, R.A. Kroczek, ICOS is an inducible T-cell co-stimulator structurally and functionally related to CD28, Nature 397 (6716) (1999) 263–266.
[22] H. Ueno, J. Banchereau, C.G. Vinuesa, Pathophysiology of T follicular helper cells in humans and mice, Nat. Immunol. 16 (2) (2015) 142–152.
[23] C.G. Vinuesa, S.G. Tangye, B. Moser, C.R. MacKay, Follicular B helper T cells in antibody responses and autoimmunity, Nat. Rev. Immunol. 5 (11) (2005) 853–865.
[24] H. Xu, X. Li, D. Liu, J. Li, X. Zhang, X. Chen, S. Hou, L. Peng, C. Xu, W. Liu, L. Zhang, H. Qi, Follicular T-helper cell recruitment governed by bystander B cells and ICOS-driven motility, Nature 496 (7446) (2013) 523–527.
[25] D. Liu, H. Xu, C. Shih, Z. Wan, X. Ma, W. Ma, D. Luo, H. Qi, T-B-cell entanglement and ICOSL-driven feed-forward regulation of germinal Centre reaction, Nature 517 (7533) (2015) 214–218.
[26] J.P. Weber, F. Fuhrmann, R.K. Feist, A. Lahmann, M.S. Al Baz, L.J. Gentz, D. Vu Van, H.W. Mages, C. Haftmann, R. Riedel, J.R. Grun, W. Schuh, R.A. Kroczek, A. Radbruch, M.F. Mashreghi, A. Hutloff, ICOS maintains the T follicular helper cell phenotype by down-regulating Kruppel-like factor 2, J. Exp. Med. 212 (2) (2015) 217–233.
[27] D.J. Wikenheiser, J.S. Stumhofer, ICOS co-stimulation: friend or foe? Front. Immunol. 7 (2016) 304.
[28] Y. Agata, A. Kawasaki, H. Nishimura, Y. Ishida, T. Tsubata, H. Yagita, T. Honjo, Expression of the PD-1 antigen on the surface of stimulated mouse T and B lymphocytes, Int. Immunol. 8 (5) (1996) 765–772.
[29] D. Allen, T. Simon, F. Sablitzky, K. Rajewsky, A. Cumano, Antibody engineering for the analysis of affinity maturation of an anti-hapten response, EMBO J. 7 (7) (1988) 1995–2001.
[30] C. Huang, K. Hatzi, A. Melnick, Lineage-specific functions of Bcl-6 in immunity and inflammation are mediated by distinct biochemical mechanisms, Nat. Immunol. 14 (4) (2013) 380–388.
[31] K.G.C. Smith, The extent of affinity maturation differs between the memory and antibody-forming cell compartments in the primary immune response, EMBO J. 16 (11) (1997) 2996–3006.
[32] S. Hardtke, Balanced expression of CXCR5 and CCR7 on follicular T helper cells determines their transient positioning to lymph node follicles and is essential for efficient B-cell help, Blood 106 (6) (2005) 1924–1931.
[33] H. Xu, X. Li, D. Liu, J. Li, X. Zhang, X. Chen, S. Hou, L. Peng, C. Xu, W. Liu, L. Zhang, H. Qi, Follicular T-helper cell recruitment governed by bystander B cells and ICOS-driven motility, Nature 496 (7446) (2013) 523–527.
[34] A.H. Tan, S.C. Wong, K.P. Lam, Regulation of mouse inducible costimulator (ICOS) expression by Fyn-NFATc2 and ERK signaling in T cells, J. Biol. Chem. 281 (39) (2006) 28666–28678.
[35] T. Okazaki, T. Honjo, The PD-1–PD-L pathway in immunological tolerance, Trends Immunol. 27 (4) (2006) 195–201.
[36] M.E. Keir, M.J. Butte, G.J. Freeman, A.H. Sharpe, PD-1 and its ligands in tolerance and immunity, Annu. Rev. Immunol. 26 (1) (2008) 677–704.
[37] S. Chikuma, S. Terawaki, T. Hayashi, R. Nabeshima, T. Yoshida, S. Shibayama,

T. Okazaki, T. Honjo, PD-1-mediated suppression of IL-2 production induces CD8+ T cell Anergy in vivo, J. Immunol. 182 (11) (2009) 6682–6689.
[38] H.T. Jin, A.C. Anderson, W.G. Tan, E.E. West, S.J. Ha, K. Araki, G.J. Freeman, V.K. Kuchroo, R. Ahmed, Cooperation of Tim-3 and PD-1 in CD8 T-cell exhaustion during chronic viral infection, Proc. Natl. Acad. Sci. 107 (33) (2010) 14733–14738.
[39] C. Robert, G.V. Long, B. Brady, C. Dutriaux, M. Maio, L. Mortier, J.C. Hassel, P. Rutkowski, C. McNeil, E. Kalinka-Warzocha, K.J. Savage, M.M. Hernberg, C. Lebbé, J. Charles, C. Mihalcioiu, V. Chiarion-Sileni, C. Mauch, F. Cognetti, A. Arance, H. Schmidt, D. Schadendorf, H. Gogas, L. Lundgren-Eriksson, C. Horak, B. Sharkey, I.M. Waxman, V. Atkinson, P.A. Ascierto, Nivolumab in previously untreated melanoma without BRAF mutation, N. Engl. J. Med. 372 (4) (2015) 320–330.
[40] H. Nishimura, M. Nose, H. Hiai, N. Minato, T. Honjo, Development of lupus-like autoimmune diseases by disruption of the PD-1 gene encoding an ITIM motif-carrying immunoreceptor, Immunity 11 (2) (1999) 141–151.
[41] H. Nishimura, T. Okazaki, Y. Tanaka, K. Nakatani, M. Hara, A. Matsumori, S. Sasayama, A. Mizoguchi, H. Hiai, N. Minato, T. Honjo, Autoimmune dilated cardiomyopathy in PD-1 receptor-deficient mice, Science 291 (5502) (2001) 319–322.
[42] S. Kasagi, S. Kawano, T. Okazaki, T. Honjo, A. Morinobu, S. Hatachi, K. Shimatani, Y. Tanaka, N. Minato, S. Kumagai, Anti-programmed cell death 1 antibody reduces CD4+PD-1+ T cells and relieves the lupus-like nephritis of NZB/W F1 mice, J. Immunol. 184 (5) (2010) 2337–2347.
[43] S. Crotty, Follicular helper CD4 T cells (TFH), Annu. Rev. Immunol. 29 (2011) 621–663.
[44] G.D. Victora, M.C. Nussenzweig, Germinal centers, Annu. Rev. Immunol. 30 (2012) 429–457.
[45] P.T. Sage, L.M. Francisco, C.V. Carman, A.H. Sharpe, The receptor PD-1 controls follicular regulatory T cells in the lymph nodes and blood, Nat. Immunol. 14 (2) (2013) 152–161.
[46] X. Xiao, X.M. Lao, M.M. Chen, R.X. Liu, Y. Wei, F.Z. Ouyang, D.P. Chen, X.Y. Zhao, Q. Zhao, X.F. Li, C.L. Liu, L. Zheng, D.M. Kuang, PD-1hi identifies a novel regulatory B-cell population in human hepatoma that promotes disease progression, Cancer Discov. 6 (5) (2016) 546–559.
[47] A.R. Khan, E. Hams, A. Floudas, T. Sparwasser, C.T. Weaver, P.G. Fallon, PD-L1hi B cells are critical regulators of humoral immunity, Nat. Commun. 6 (2015) 5997.
[48] C. King, S.G. Tangye, C.R. MacKay, T follicular helper (TFH) cells in normal and dysregulated immune responses, Annu. Rev. Immunol. 26 (2008) 741–766.